Random walks on complex networks under time-dependent stochastic resetting

Hanshuang Chen* and Yanfei Ye
School of Physics and Optoelectronic Engineering, Anhui University, Hefei 230601, China

(Received 31 July 2022; accepted 5 October 2022; published 31 October 2022)

We study discrete-time random walks on networks subject to a time-dependent stochastic resetting, where the walker either hops randomly between neighboring nodes with a probability $1-\phi(a)$ or is reset to a given node with a complementary probability $\phi(a)$. The resetting probability $\phi(a)$ depends on the time a since the last reset event (also called a, the age of the walker). Using the renewal approach and spectral decomposition of the transition matrix, we formulate the stationary occupation probability of the walker at each node and the mean first passage time between two arbitrary nodes. Concretely, we consider two different time-dependent resetting protocols that are both exactly solvable. One is that $\phi(a)$ is a step-shaped function of a and the other one is that $\phi(a)$ is a rational function of a. We demonstrate the theoretical results on several different networks, also validated by numerical simulations, and find that the time-modulated resetting protocols can be more advantageous than the constant-probability resetting in accelerating the completion of a target search process.

DOI: 10.1103/PhysRevE.106.044139

I. INTRODUCTION

Since the seminal work by Evans and Majumdar [1], random walks subject to resetting processes have received growing attention in the past decade (see [2] for a recent review). The walker is stochastically interrupted and reset to the initial position, and the random process is then restarted. Interestingly, the occupation probability at stationarity is strongly altered. The mean time to reach a given target for the first time can become finite and be minimized with respect to the resetting rate. Some extensions have been made in the field, such as spatially [3] or temporally [4–8] dependent resetting rate, higher dimensions [9], complex geometries [10–13], noninstantaneous resetting [14–17], in the presence of external potential [17–19], other types of Brownian motion such as run-and-tumble particles [20–22], active particles [23,24], constrained Brownian particle [25], and so on [26]. These nontrivial findings have triggered enormous recent activity in the field, including statistical physics [9,27–37], stochastic thermodynamics [38–40], chemical and biological processes [41–45], extremal statistics [46–48], optimal control theory [49], and single-particle experiments [50,51].

However, the impact of resetting on random walks on networked systems has received only a small amount of attention [52–57]. Random walks on complex networks is a simple but very important model [58–60]. It not only underlies many important dynamical processes on networked systems, such as epidemic spreading [61–63], population extinction [64,65], neuronal firing [66], and consensus formation [67], but also finds a broad range of applications, such as community detection [68–70], human mobility [71–73], and ranking and searching on the web [59,74–77]. Random walks on networks under resetting have many applications in computer science and physics. For instance, label propagation in machine learning algorithms [78], or the famous PageRank [79], can be interpreted as a random walker with uniform resetting probability to all the nodes of the network. Human and animal mobility consists of a mixture of short-range moves with intermittent long-range moves where an agent relocates to a new place and then starts local moves [80–82]. Until recently, Riascos *et al.* [83] established relationships between the random walk dynamics with resetting to one node and the spectral representation of the transition matrix in the absence of resetting [84]. Furthermore, they discussed the condition under which resetting becomes advantageous to reduce the mean first passage time (MFPT) [85]. Subsequently, the result was generalized to the case when multiple resetting nodes exist [86,87]. In a recent work, we have generalized the constant resetting probability to the case when the resetting probability is node dependent [88].

In this paper, we consider a different generalization of the resetting random walks on networks: a time-dependent resetting probability. This generalization is quite natural in the context of target search. When searching for a target, it is unlikely to restart at the beginning. But as time elapses without success, it is more likely to return to the original point and restart the search process. We should note that for continuous-time random walks on one-dimensional space, a similar problem has been considered in several recent works, including nonexponential waiting times between successive resets [4,6,7] and the time-dependent resetting rate [5]. The case of a resetting rate that depends on the absolute time elapsed from the beginning of the process was considered in [8]. In the present work, we focus on discrete-time random walks on arbitrary networks subject to a time-dependent resetting probability $\phi(a)$, where a refers to the time since the last reset event (or, as we call it, the age of the walker), rather

*chenhshf@ahu.edu.cn

than the absolute time from the initial condition. This means that when a reset happens, the walker no longer remembers what happened before resetting and thus the process is still Markovian. First of all, we formulate the occupation probability distribution and the MFPT for a general choice of $\phi(a)$ by the renewal approach combined with the spectrum properties of the transition matrix. We then consider two exactly solvable examples for the settings of $\phi(a)$. The first example is that $\phi(a)$ is a step-shaped function where the resetting probability switches from one value to another one at $a = a_c$. The second one is that $\phi(a) = \frac{a}{a+a_c}$ is a strictly increasing function from zero as a increases. The theoretical and simulation results show that such time-modulated resetting protocols are able to expedite the completion of a target search compared with the constant-probability resetting.

II. MODEL

Consider a walker that performs discrete-time random walks on an undirected and unweighted network of size N [58]. At each time step, the walker either hops between two neighboring nodes with a probability $1 - \phi(a)$ or is reset to a given node with a complementary probability $\phi(a)$, where a denotes the age of the walker determined by an internal clock carried by the walker itself. For the former, the walker jumps from the current node to one of its neighboring nodes with equal probabilities, in the sense that the transition probability from node i to node j can be written as $W_{ij} = A_{ij}/k_i$, where A_{ij} is the element of adjacency matrix of the underlying network, and $k_i = \sum_{j=1}^{N} A_{ij}$ is the degree of node i. Meanwhile, the age of the walker is increased by one: $a \to a + 1$. For the latter, the walker is reset to node r (called the resetting node) and its age is simultaneously reinitialized to zero, $a \to 0$.

III. OCCUPATION PROBABILITY

Let us denote by $P_{ij}(t)$ the probability to find the walker at node j at time t providing it has started from node i. $P_{ij}(t)$ satisfies a first renewal equation [5,19,31,87],

$$P_{ij}(t) = \Phi(t)P^0_{ij}(t) + \sum_{t'=0}^{t} \Psi(t')P_{rj}(t - t'), \tag{1}$$

where

$$\Phi(t) = \prod_{a=1}^{t} [1 - \phi(a)] \tag{2}$$

is the probability of no reset taking place up to time t, and

$$\Psi(t) = \begin{cases} \Phi(t-1)\phi(t), & t \geqslant 1 \\ 0, & t = 0 \end{cases} \tag{3}$$

is the probability of the first reset taking place at time t. $P^0_{ij}(t)$ is the occupation probability of the walker in the absence of resetting processes [59], given by (see Appendix A for details)

$$P^0_{ij}(t) = \sum_{\ell=1}^{N} \lambda^t_\ell \langle i|\phi_\ell\rangle\langle\bar{\phi}_\ell|j\rangle, \tag{4}$$

where λ_ℓ is the ℓth eigenvalue of the transition matrix $\boldsymbol{W}$, and the corresponding left eigenvector and right eigenvector are, respectively, $\langle\bar{\phi}_\ell|$ and $|\phi_\ell\rangle$, satisfying $\langle\bar{\phi}_\ell|\phi_m\rangle = \delta_{\ell m}$ and $\sum_{\ell=1}^{N} |\phi_\ell\rangle\langle\bar{\phi}_\ell| = \boldsymbol{I}$. $|i\rangle$ denotes the canonical base with all its components equal to zero, except the ith one, which is equal to 1. The first term on the right-hand side of Eq. (1) accounts for the walker never reset up to time t, and the second term accounts for the walker reset at time t' for the first time, after which the process starts anew from the resetting node r for the remaining time $t - t'$.

Let $\kappa_{ij}(t) = \Phi(t)P^0_{ij}(t)$, and take the discrete-time Laplace transform for Eq. (1), $\tilde{f}(s) = \sum_{t=0}^{\infty} e^{-st} f(t)$, which yields

$$\tilde{P}_{ij}(s) = \tilde{\kappa}_{ij}(s) + \tilde{\Psi}(s)\tilde{P}_{rj}(s), \tag{5}$$

from which one readily obtains

$$\tilde{P}_{ij}(s) = \tilde{\kappa}_{ij}(s) + \frac{\tilde{\Psi}(s)}{1 - \tilde{\Psi}(s)}\tilde{\kappa}_{rj}(s). \tag{6}$$

In the specific case where the resetting node is the same as the original node, $r = i$, Eq. (6) simplifies to

$$\tilde{P}_{ij}(s) = \frac{\tilde{\kappa}_{ij}(s)}{1 - \tilde{\Psi}(s)}. \tag{7}$$

By inverting Eq. (6), one obtains the occupation probability $P_{ij}(t)$. However, in most instances, the inverse transform of Eq. (6) is almost impossible to reach. Instead, one can take the limit,

$$P_j(\infty) = \lim_{s\to 0} (1 - e^{-s})\tilde{P}_{ij}(s), \tag{8}$$

to obtain the stationary occupation probability of the walker at each node.

IV. SURVIVAL PROBABILITY

Let us suppose that there is a target located at node j. Once it visits the target node, the walker will be absorbed immediately and the process will be terminated. Let us denote by $Q_{ij}(t)$ the survival probability of the walker at time t, providing that the walker has started from node i. $Q_{ij}(t)$ satisfies a first renewal equation [5,19,31,87],

$$Q_{ij}(t) = \Phi(t)Q^0_{ij}(t) + (1 - \delta_{jr}) \times \sum_{t'=1}^{t} \Psi(t')Q^0_{ij}(t' - 1)Q_{rj}(t - t'), \tag{9}$$

where $Q^0_{ij}(t)$ denotes the survival probability in the absence of resetting processes (see Appendix B for details). The first term on the right-hand side of Eq. (9) corresponds to the case where there is no resetting event at all up to time t, which occurs with probability $\Phi(t)$. The second term accounts for the event where the first resetting takes place at time t', which occurs with probability $\Psi(t')$. Before the first resetting, the walker survives with the probability $Q^0_{ij}(t' - 1)$, after which the walker survives with the probability $Q_{rj}(t - t')$. If the resetting node is the same as the target node, $r = j$, the walker is immediately absorbed as soon as it is reset. Therefore, the prefactor $1 - \delta_{jr}$ ensures the second term on the right-hand side of Eq. (9) vanishes when $r = j$.

Let $\chi_{ij}(t) = \Phi(t)Q^0_{ij}(t)$, $\eta_{ij}(t) = \Psi(t)Q^0_{ij}(t - 1)$ [noting that $\Psi(0) = 0$], and take the Laplace transform for Eq. (9),

which yields,

$$\tilde{Q}_{ij}(s) = \tilde{\chi}_{ij}(s) + (1-\delta_{jr})\tilde{\eta}_{ij}(s)\tilde{Q}_{rj}(s). \tag{10}$$

From Eq. (10), one can explicitly obtain

$$\tilde{Q}_{ij}(s) = \tilde{\chi}_{ij}(s) + \frac{(1-\delta_{jr})\tilde{\eta}_{ij}(s)}{1-(1-\delta_{jr})\tilde{\eta}_{rj}(s)}\tilde{\chi}_{rj}(s). \tag{11}$$

For the special case when the resetting node coincides with the original node, $r = i$, Eq. (11) simplifies to

$$\tilde{Q}_{ij}(s) = \frac{\tilde{\chi}_{ij}(s)}{1-(1-\delta_{ij})\tilde{\eta}_{ij}(s)}. \tag{12}$$

The MFPT from node i to node j is given by

$$\begin{aligned}\langle T_{ij}\rangle &= \tilde{Q}_{ij}(0) \\ &= \tilde{\chi}_{ij}(0) + \frac{(1-\delta_{jr})\tilde{\eta}_{ij}(0)}{1-(1-\delta_{jr})\tilde{\eta}_{rj}(0)}\tilde{\chi}_{rj}(0).\end{aligned} \tag{13}$$

For the case when the resetting node is the same as the original node, $r = i$, Eq. (13) reduces to

$$\langle T_{ij}\rangle = \frac{\tilde{\chi}_{ij}(0)}{1-(1-\delta_{ij})\tilde{\eta}_{ij}(0)}. \tag{14}$$

V. CONSTANT-PROBABILITY RESETTING

For completeness, we first consider the case when the resetting probability at each time step is a constant, $\phi(a) = \gamma$, which is independent of the age of the walker. In this case, we have $\Phi(t) = (1-\gamma)^t$, $\Psi(t) = (1-\gamma)^{t-1}\gamma$ for $t \geqslant 1$, and $\Psi(0) = 0$ for $t = 0$,

$$\kappa_{ij}(t) = \Phi(t)P^0_{ij}(t) = \sum_{\ell=1}^{N}\lambda_\ell^t(1-\gamma)^t\langle i|\phi_\ell\rangle\langle\bar{\phi}_\ell|j\rangle. \tag{15}$$

Taking the Laplace transform for $\Psi(t)$ and $\kappa_{ij}(t)$, we have

$$\tilde{\Psi}(s) = \frac{\gamma e^{-s}}{1-(1-\gamma)e^{-s}} \tag{16}$$

and

$$\tilde{\kappa}_{ij}(s) = \sum_{\ell=1}^{N}\frac{1}{1-\lambda_\ell(1-\gamma)e^{-s}}\langle i|\phi_\ell\rangle\langle\bar{\phi}_\ell|j\rangle. \tag{17}$$

Substituting Eqs. (16) and (17) into Eq. (6), we have

$$\begin{aligned}\tilde{P}_{ij}(s) = \frac{\langle\bar{\phi}_1|j\rangle}{1-e^{-s}} &+ \sum_{\ell=2}^{N}\frac{1}{1-\lambda_\ell(1-\gamma)e^{-s}}\langle i|\phi_\ell\rangle\langle\bar{\phi}_\ell|j\rangle \\ &+ \frac{\gamma e^{-s}}{1-e^{-s}}\sum_{\ell=2}^{N}\frac{1}{1-\lambda_\ell(1-\gamma)e^{-s}}\langle r|\phi_\ell\rangle\langle\bar{\phi}_\ell|j\rangle.\end{aligned} \tag{18}$$

Taking the inverse transform for Eq. (18), we have

$$\begin{aligned}P_{ij}(t) = \langle\bar{\phi}_1|j\rangle &+ \sum_{\ell=2}^{N}\lambda_\ell^t(1-\gamma)^t\langle i|\phi_\ell\rangle\langle\bar{\phi}_\ell|j\rangle \\ &+ \gamma\sum_{\ell=2}^{N}\frac{1-\lambda_\ell^t(1-\gamma)^t}{1-\lambda_\ell(1-\gamma)}\langle r|\phi_\ell\rangle\langle\bar{\phi}_\ell|j\rangle.\end{aligned} \tag{19}$$

In stationarity, $t \to \infty$, $\lambda_\ell^t \to 0$ for $\ell = 2, \ldots, N$, we get to the stationary occupation probability in the presence of constant-probability resetting processes,

$$P_j(\infty) = \langle\bar{\phi}_1|j\rangle + \gamma\sum_{\ell=2}^{N}\frac{\langle r|\phi_\ell\rangle\langle\bar{\phi}_\ell|j\rangle}{1-\lambda_\ell(1-\gamma)}. \tag{20}$$

The first term on the right-hand side of Eq. (20) is the stationary occupation probability in the absence of resetting [59], and the second term is a nonequilibrium contribution due to the resetting processes.

In the following, we will derive the MFPT for the case of a constant resetting probability. To that end, we take the Laplace transform for $\chi_{ij}(t)$ and $\eta_{ij}(t)$, which yields

$$\begin{aligned}\tilde{\chi}_{ij}(s) &= \sum_{t=0}^{\infty}e^{-st}\Phi(t)Q^0_{ij}(t) = \sum_{t=0}^{\infty}e^{-s't}Q^0_{ij}(t) \\ &= \tilde{Q}^0_{ij}(s')\end{aligned} \tag{21}$$

and

$$\begin{aligned}\tilde{\eta}_{ij}(s) &= \sum_{t=1}^{\infty}e^{-st}\Psi(t)Q^0_{ij}(t-1) = \gamma e^{-s}\sum_{t=0}^{\infty}e^{-s't}Q^0_{ij}(t) \\ &= \gamma e^{-s}\tilde{Q}^0_{ij}(s'),\end{aligned} \tag{22}$$

where $s' = s - \ln(1-\gamma)$. Substituting Eqs. (21) and (22) into Eq. (11), we have

$$\tilde{Q}_{ij}(s) = \tilde{Q}^0_{ij}(s') + \frac{(1-\delta_{jr})\gamma e^{-s}\tilde{Q}^0_{ij}(s')}{1-(1-\delta_{jr})\gamma e^{-s}\tilde{Q}^0_{rj}(s')}\tilde{Q}^0_{rj}(s'). \tag{23}$$

The MFPT is given by Eq. (13) combined with Eq. (23),

$$\begin{aligned}\langle T_{ij}\rangle = \tilde{Q}^0_{ij}[-\ln(1-\gamma)] &\\ + \frac{(1-\delta_{jr})\gamma\tilde{Q}^0_{ij}[-\ln(1-\gamma)]}{1-(1-\delta_{jr})\gamma\tilde{Q}^0_{rj}[-\ln(1-\gamma)]}&\tilde{Q}^0_{rj}[-\ln(1-\gamma)].\end{aligned} \tag{24}$$

In Appendix B, we have derived the survival probability in the Laplace domain for the standard random walks without resetting [see Eq. (B5)], from which we obtain

$$\tilde{Q}^0_{ij}[-\ln(1-\gamma)] = \frac{\sum_{\ell=2}^{N}\frac{\langle j|\phi_\ell\rangle\langle\bar{\phi}_\ell|j\rangle - \langle i|\phi_\ell\rangle\langle\bar{\phi}_\ell|j\rangle}{1-\lambda_\ell(1-\gamma)} + \delta_{ij}}{\langle\bar{\phi}_1|j\rangle + \gamma\sum_{\ell=2}^{N}\frac{\langle j|\phi_\ell\rangle\langle\bar{\phi}_\ell|j\rangle}{1-\lambda_\ell(1-\gamma)}}. \tag{25}$$

Substituting Eq. (25) into Eq. (24) and combining Eq. (20), we have

$$\langle T_{ij}\rangle = \frac{1}{P_j(\infty)}\left[\sum_{\ell=2}^{N}\frac{\langle j|\phi_\ell\rangle\langle\bar{\phi}_\ell|j\rangle - \langle i|\phi_\ell\rangle\langle\bar{\phi}_\ell|j\rangle}{1-\lambda_\ell(1-\gamma)} + \delta_{ij}\right]. \tag{26}$$

Equations (20) and (26) have been derived in Ref. [83] using a different method. These results were also generalized to the case when multiple resetting nodes exist [86,87]. The main contribution of the present work is the analysis of time-dependent resetting probability, which will be presented in the following.

VI. TIME-DEPENDENT RESETTING

A. Step-shaped resetting probability

We consider the resetting probability as a step-shaped function of a,

$$\phi(a) = \begin{cases} \gamma_1, & a \leqslant a_c \\ \gamma_2, & a > a_c, \end{cases} \tag{27}$$

where a_c is a characteristic age that controls the time when the value of the resetting probability is switched. According to Eqs. (2) and (3), we have

$$\Phi(t) = \begin{cases} (1-\gamma_1)^t, & t \leqslant a_c \\ (1-\gamma_1)^{a_c}(1-\gamma_2)^{t-a_c}, & t > a_c \end{cases} \tag{28}$$

and

$$\Psi(t) = \begin{cases} (1-\gamma_1)^{t-1}\gamma_1, & t \leqslant a_c \\ (1-\gamma_1)^{a_c}(1-\gamma_2)^{t-a_c-1}\gamma_2, & t > a_c, \end{cases} \tag{29}$$

for $t \geqslant 1$, and $\Psi(0) = 0$. Performing the Laplace transform for $\Psi(t)$ and $\kappa_{ij}(t) = \Phi(t)P_{ij}^0(t)$, we have

$$\tilde{\Psi}(s) = \frac{\gamma_1 e^{-s}[1 - e^{-sa_c}(1-\gamma_1)^{a_c}]}{1-(1-\gamma_1)e^{-s}} + \frac{\gamma_2 e^{-s(a_c+1)}(1-\gamma_1)^{a_c}}{1-(1-\gamma_2)e^{-s}} \tag{30}$$

and

$$\tilde{\kappa}_{ij}(s) = \sum_{\ell=1}^{N}\left[\frac{1 - e^{-s(1+a_c)}\lambda_\ell^{1+a_c}(1-\gamma_1)^{1+a_c}}{1-\lambda_\ell(1-\gamma_1)e^{-s}} + \frac{e^{-s(1+a_c)}\lambda_\ell^{1+a_c}(1-\gamma_1)^{a_c}(1-\gamma_2)}{1-\lambda_\ell(1-\gamma_2)e^{-s}}\right]\langle i|\phi_\ell\rangle\langle\bar{\phi}_\ell|j\rangle. \tag{31}$$

Substituting Eqs. (30) and (31) into Eq. (8), we obtain the stationary occupation probability,

$$P_j(\infty) = \langle\bar{\phi}_1|j\rangle + \sum_{\ell=2}^{N}\frac{\gamma_1\gamma_2\left[1-(1-\gamma_2)\lambda_\ell + (1-\gamma_1)^{a_c}(\gamma_1-\gamma_2)\lambda_\ell^{a_c+1}\right]}{[1-(1-\gamma_1)\lambda_\ell][1-(1-\gamma_2)\lambda_\ell][(1-\gamma_1)^{a_c}(\gamma_1-\gamma_2)+\gamma_2]}\langle r|\phi_\ell\rangle\langle\bar{\phi}_\ell|j\rangle. \tag{32}$$

If $\gamma_1 = \gamma_2$, Eq. (32) recovers to the result of Eq. (20) when the resetting probability is a constant.

In order to obtain the MFPT by Eq. (13), we need to derive the expression of $\tilde{\chi}_{ij}(s)$ and $\tilde{\eta}_{ij}(s)$ at $s = 0$. In Appendix C, we have derived the survival probability for the standard random walks; see Eq. (C3). Substituting Eq. (C3) into the definitions of $\chi_{ij}(t)$ and $\eta_{ij}(t)$, and then taking the sum over t, we obtain

$$\tilde{\chi}_{ij}(0) = \sum_{\ell=1}^{N}\left[\frac{1-(1-\gamma_1)^{a_c+1}\left[\zeta_\ell^{(j)}\right]^{a_c+1}}{1-(1-\gamma_1)\zeta_\ell^{(j)}} + \frac{(1-\gamma_1)^{a_c}(1-\gamma_2)\left[\zeta_\ell^{(j)}\right]^{a_c+1}}{1-(1-\gamma_2)\zeta_\ell^{(j)}}\right]\langle i|\psi_\ell^{(j)}\rangle\langle\bar{\psi}_\ell^{(j)}|\mathbf{1}\rangle \tag{33}$$

and

$$\tilde{\eta}_{ij}(0) = \sum_{\ell=1}^{N}\left[\frac{\gamma_1\left[1-(1-\gamma_1)^{a_c}\left[\zeta_\ell^{(j)}\right]^{a_c}\right]}{1-(1-\gamma_1)\zeta_\ell^{(j)}} + \frac{(1-\gamma_1)^{a_c}\gamma_2\left[\zeta_\ell^{(j)}\right]^{a_c}}{1-(1-\gamma_2)\zeta_\ell^{(j)}}\right]\langle i|\psi_\ell^{(j)}\rangle\langle\bar{\psi}_\ell^{(j)}|\mathbf{1}\rangle, \tag{34}$$

for $i \neq j$. Here, $|\mathbf{1}\rangle = (1,\ldots,1)^\top$ is an N-dimensional right vector with all components equal to one. $\zeta_\ell^{(j)}$ is the ℓth eigenvalue of the matrix $\boldsymbol{W}_j$, and the associated left and right eigenvectors are, respectively, $\langle\bar{\psi}_\ell^{(j)}|$ and $|\psi_\ell^{(j)}\rangle$, satisfying $\langle\bar{\psi}_\ell^{(j)}|\psi_m^{(j)}\rangle = \delta_{\ell m}$ and $\sum_{\ell=1}^{N}|\psi_\ell^{(j)}\rangle\langle\bar{\psi}_\ell^{(j)}| = \boldsymbol{I}$. The matrix $\boldsymbol{W}_j$ is obtained by letting all the entries in the jth row and the jth column of $\boldsymbol{W}$ equal zero (see Appendix C for details).

Considering the following special case: $\gamma_1 = 0$, $\gamma_2 = \gamma$. Equation (32) is simplified to

$$P_j(\infty) = \langle\bar{\phi}_1|j\rangle + \gamma\sum_{\ell=2}^{N}\frac{1-\lambda_\ell+\gamma\lambda_\ell(1-\lambda_\ell^{a_c})}{(1+\gamma a_c)(1-\lambda_\ell)[1-(1-\gamma)\lambda_\ell]} \times \langle r|\phi_\ell\rangle\langle\bar{\phi}_\ell|j\rangle. \tag{35}$$

Again, the first term on the right-hand side of Eq. (35) corresponds to the stationary occupation distribution of the standard random walk, and the second term to a nonequilibrium contribution due to resetting. For $a_c \to \infty$, the second term in Eq. (35) vanishes and thus recovers to the result when the resetting is absent.

Equations (33) and (34) for $\gamma_1 = 0$ and $\gamma_2 = \gamma$ can be simplified to

$$\tilde{\chi}_{ij}(0) = \sum_{\ell=1}^{N}\left\{\frac{1-\left[\zeta_\ell^{(j)}\right]^{1+a_c}}{1-\zeta_\ell^{(j)}} + \frac{(1-\gamma)\left[\zeta_\ell^{(j)}\right]^{1+a_c}}{1-(1-\gamma)\zeta_\ell^{(j)}}\right\} \times \langle i|\psi_\ell^{(j)}\rangle\langle\bar{\psi}_\ell^{(j)}|\mathbf{1}\rangle \tag{36}$$

and

$$\tilde{\eta}_{ij}(0) = \gamma\sum_{\ell=1}^{N}\frac{\left[\zeta_\ell^{(j)}\right]^{a_c}}{1-(1-\gamma)\zeta_\ell^{(j)}}\langle i|\psi_\ell^{(j)}\rangle\langle\bar{\psi}_\ell^{(j)}|\mathbf{1}\rangle. \tag{37}$$

We should note that for $a_c = 0$, the model recovers to the case of the resetting with constant probability. For $a_c \to \infty$, it corresponds to the standard random walks without resetting.

To demonstrate the theoretical results, we first consider a ring network with the size $N = 50$ [see the inset of Fig. 1(a)]. In Fig. 1(a), we show the stationary occupation probability

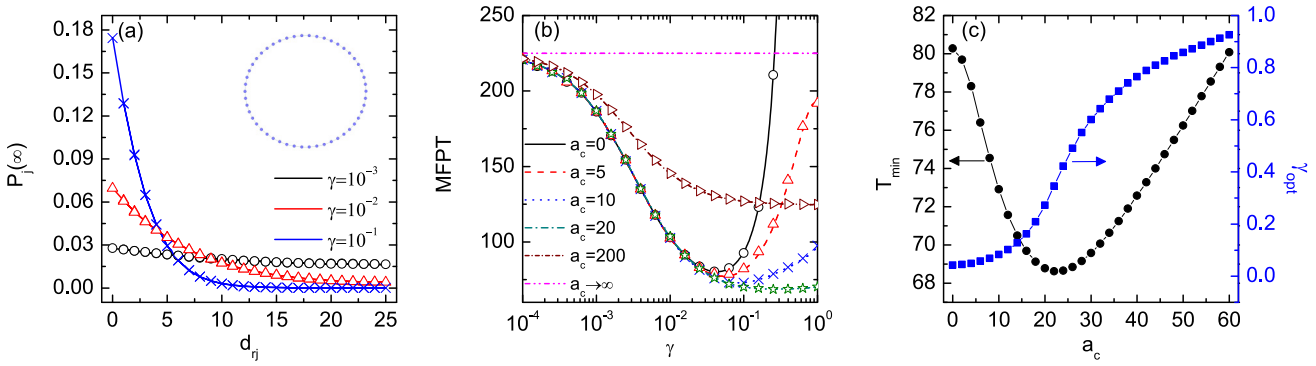

FIG. 1. Results for the step-shaped resetting [see Eq. (27) for $\gamma_1 = 0$ and $\gamma_2 = \gamma$] on a ring network of $N = 50$ [see the inset of (a)]. The resetting node is set to be the same as the starting node, $r = i$. (a) The stationary occupation probability $P_j(\infty)$ at node j as a function of the distance d_{rj} to the resetting node r for different γ. The characteristic age is fixed at $a_c = 10$. (b) The MFPT as a function of the resetting probability γ for different a_c. Lines and symbols correspond to the theory and simulation results, respectively. Note that $a_c = 0$ corresponds to the case of the resetting with a constant probability γ, and $a_c \to \infty$ to the case without resetting. (c) The minimum $T_{\min}$ of the MFPT and the corresponding optimal resetting probability $\gamma_{\rm opt}$ as a function of a_c. The distance between the starting node and the target node is $d_{ij} = 5$.

at each node as a function of the distance to the resetting node for three different resetting probabilities γ, where the characteristic age is fixed at $a_c = 10$. To validate the theoretical results, we also performed the Monte Carlo simulations and found that there is a good agreement between theory and simulation. In all simulations, we have used 10^7 time steps to calculate the stationary occupation probability. The stationary occupation probability decreases monotonically with increases to the distance to the resetting node. For a larger resetting probability, the walker has a larger probability of staying near the resetting position. In Fig. 1(b), we show the MFPT as a function of γ for several different values of a_c, where the distance between the starting node and the target node is fixed at $d_{ij} = 5$, and the resetting node is set to be the same as the starting node. Lines and symbols correspond to the theory and simulation results, respectively. In all simulations, we have used 10^5 realizations to obtain the MFPT. We can see that the MFPT under resetting shows a nonmonotonic dependence on γ. There exists an optimal resetting probability $\gamma_{\rm opt}$ at which the MFPT attains a minimum $T_{\min}$. In a wide range of γ, the MFPT is less than that for the case without resetting ($a_c \to \infty$), implying that the completion of the first passage process can be expedited by the resetting. On the other hand, such a time-dependent resetting protocol is more advantageous than the constant-probability resetting ($a_c = 0$). This is because that the minimum of MFPT is able to become smaller than that for the constant-probability resetting $T_{\min}^{\rm consreset} = 80.274$, as shown in Fig. 1(c). The MFPT shows a global minimum $T_{\min}^{*} = 68.624$ at $a_c = 22$ and $\gamma_{\rm opt} = 0.346$. The decrease in MFPT due to the step-shaped resetting is considerable.

As the second example, we consider a Cayley tree $C_{b,n}$, where b is the coordination number except for the outermost nodes and n is the number of shells. The network is generated as follows. Initially ($n = 0$), $C_{b,0}$ consists of only a central node. To form $C_{b,1}$, b nodes are created and are attached to the central node. For any $n > 1$, $C_{b,n}$ is obtained from $C_{b,n-1}$ by performing the following operation. For each boundary node of $C_{b,n-1}$, $b - 1$ nodes are generated and attached to the boundary node. The size of the Cayley tree is $N = 1 + b(2^n - 1)$. The central node is set to be the starting node and one of the outermost nodes is set to be the target node. The resetting node is the same as the starting one. In Fig. 2, we show the results on a Cayley tree $C_{3,5}$, and they are similar to those on a ring network in Fig. 1. As intuitively expected, the resetting can significantly increase the chance of the walker to visit those nodes close to the resetting node [see Fig. 2(a)]. As shown in Fig. 2(b), the MFPT first decreases and then increases with the resetting probability γ for small values of a_c, and a unique minimum MFPT, $T_{\min}$, occurs at $\gamma = \gamma_{\rm opt}$, while for relatively larger values of a_c, the MFPT decreases monotonically with γ. Interestingly, the MFPT shows a global minimum $T_{\min}^{*} = 528.94$ at a two-dimensional parameter space $(a_c, \gamma) = (22, 0.344)$ [see Fig. 2(c)]. The minimum in MFPT for the step-shaped resetting protocol is obviously smaller than that in the case of constant-probability resetting, $T_{\min}^{\rm consreset} = 596.45$.

We should note that resetting can either accelerate or hinder the MFPT depending on the positions of the starting and ending points of the walker or some parameter of the underlying model. It has been realized that a so-called restart criterion exists for the constant-probability (rate) resetting [27,28]. If the relative standard deviation of first passage time without resetting is larger than one, restart has the ability to expedite the completion of the underlying stochastic process [28,36]. Recently, such a criterion was discussed on networked systems in [85]. For the case when the resetting probability is time dependent, there is no general restart criterion at present. However, one also expects that the restart can decrease the MFPT when the variance of the first passage time without resetting is large enough.

Furthermore, we apply the step-shaped resetting protocol defined in Eq. (27) ($\gamma_1 = 0$ and $\gamma_2 = \gamma$) to more complex types of networks. First of all, we consider a Barbell network [89] of size $N = 53$ consisting of two fully connected communities (of 25 nodes each) connected by a chain of three bridge nodes [see Fig. 3(a)]. In all results shown below, we have assumed that the resetting node is the same as the starting

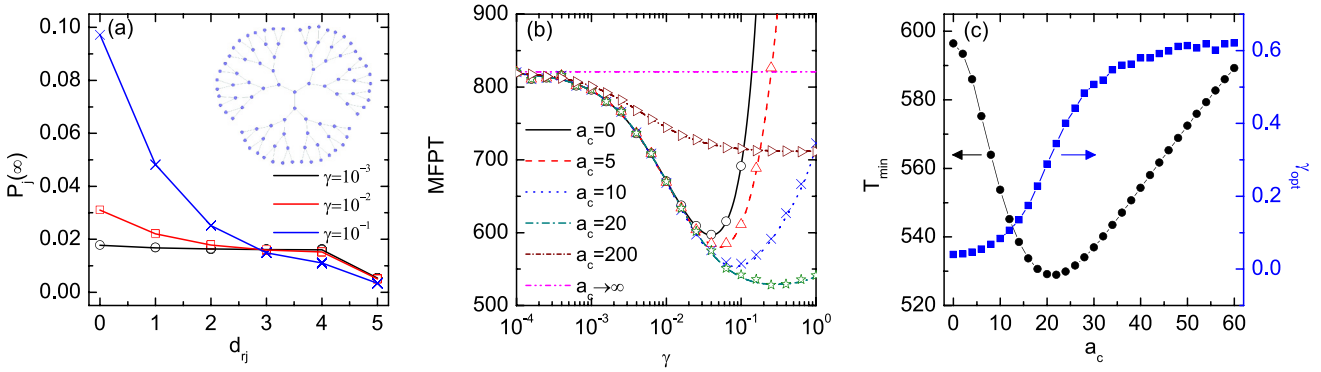

FIG. 2. Results for the step-shaped resetting [see Eq. (27) for $\gamma_1 = 0$ and $\gamma_2 = \gamma$] on a Cayley tree $C_{3,5}$ [see the inset of (a)]. The central node is set to be the resetting node. (a) The stationary occupation probability $P_j(\infty)$ at node j as a function of the distance d_{rj} to the resetting node r for different γ. The characteristic age is fixed at $a_c = 10$. (b) The MFPT as a function of the resetting probability γ for different a_c. Lines and symbols correspond to the theory and simulation results, respectively. Note that $a_c = 0$ corresponds to the case of the resetting with a constant probability γ, and $a_c \to \infty$ to the case without resetting. (c) The minimum $T_{\min}$ of the MFPT and the corresponding optimal resetting probability γ_{opt} as a function of a_c. The starting node is the same as the resetting node, and one of the outermost nodes is set to be the target node.

node. We have computed the global mean first passage time (GMFPT), defined as

$$\langle T(i)\rangle = \frac{1}{N-1}\sum_{j\neq i}^{N}\langle T_{ij}\rangle. \tag{38}$$

In fact, the GMFPT of a given starting node is the average MFPT over all possible target nodes except for the starting node itself, which is used to quantify the efficiency to explore the whole network. For the standard random walks, the walker is prone to be trapped into either of the communities, and thus makes the global search difficult. This difficulty may be overcome by resetting the walker to one of the bridge nodes. Indeed, the GMFPT can be reduced if the process is stochastically reset to one of bridge nodes; otherwise, the GMFPT always increases in the presence of resetting. These results are similar to those for the case of constant-probability resetting [83].

To show whether the time-dependent resetting is more advantageous to constant-probability resetting, we plot the

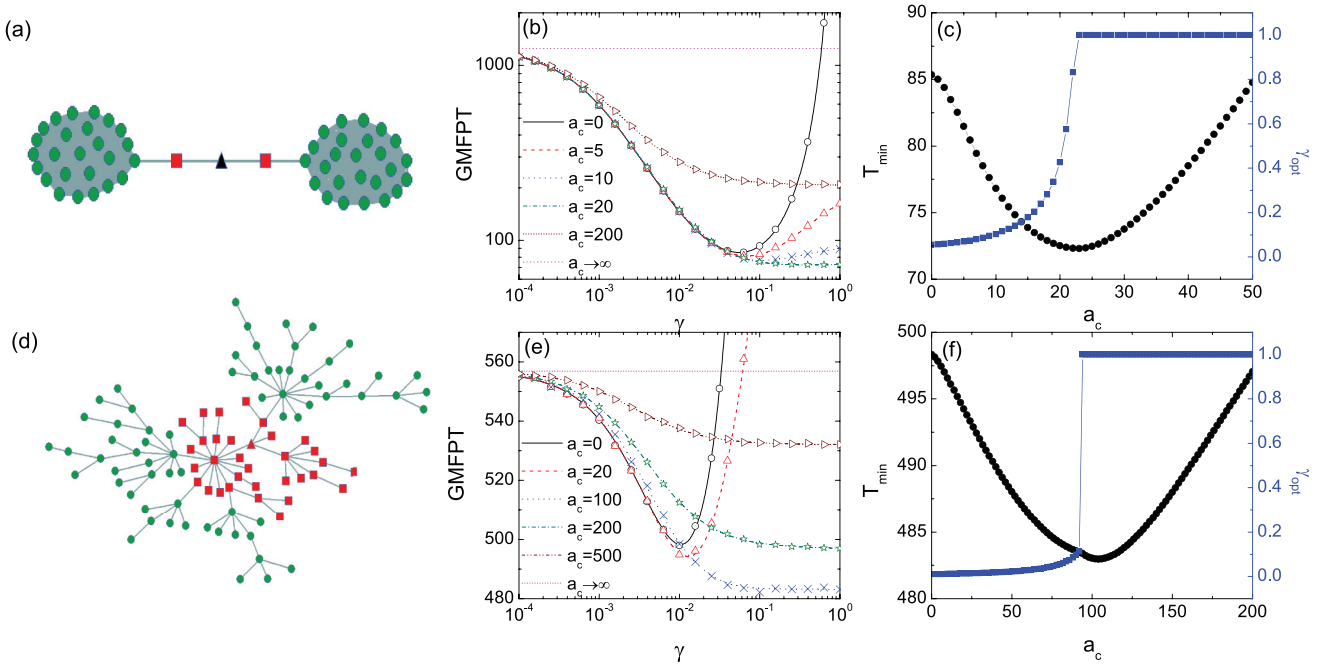

FIG. 3. Results for the step-shaped resetting [see Eq. (27) for $\gamma_1 = 0$ and $\gamma_2 = \gamma$] on a Barbell network of $N = 53$ (top panels) and on a BA scale-free network of $N = 100$ (bottom panels). The two networks are drawn in (a) and (d), respectively. (b) and (e) show the GMFPT as a function of γ for different a_c. (c) and (f) show the minimal GMFPT, $T_{\min}$, and the optimal value of γ, γ_{opt}, as a function of a_c. The resetting node is the same as the starting node, which is indicated by triangles in (a) and (d). Lines and symbols in (b) and (e) correspond to the theory and simulations, respectively.

GMFPT of the midmost bridge node as a function of γ for different a_c, as shown in Fig. 3(b). It is obvious that the GMFPT can be further reduced against the constant-probability resetting (i.e., $a_c = 0$). The minimal GMFPT, $T_{\min}$, as a function of a_c is plotted in Fig. 3(c). Correspondingly, we show the optimal value of γ as well, γ_{opt}, at which the GMFPT is minimum. $T_{\min}$ attains its minimum on two-dimensional parameter space at $(a_c, \gamma) = (23, 1)$.

We now consider a Barabási-Albert (BA) scale-free network [90] of size $N = 100$ with the average degree $\langle k \rangle = 2$; see Fig. 3(d). The GMFPT increases monotonically with γ when the process is reset to one of the peripheral nodes [circular nodes in Fig. 3(d)], whereas a minimum $T_{\min}$ may exist for the central nodes [square or triangular nodes in Fig. 3(d)]. In Fig. 3(e), we show the GMFPT as a function of γ when resetting to one of the central nodes [indicated by triangle in Fig. 3(d)]. As the previous examples show, the time-dependent resetting protocol is able to further reduce the GMFPT. In Fig. 3(f), we show $T_{\min}$ and γ_{opt} as a function of a_c. $T_{\min}$ possesses its minimum at $(a_c, \gamma) = (104, 1)$.

Meanwhile, we have checked some other types of networks, such as Erdös-Rényi random networks [91] and Watts-Strogatz small-world networks [92], and found that all the results on these networks are qualitatively the same as those reported in the present work and support the main conclusion, i.e., time-modulated resetting can be more advantageous than constant-probability resetting in reducing the mean time of the random search.

B. Anti-aging resetting probability

We consider an anti-aging resetting protocol, where the resetting probability is a strictly increasing function of the age a of the walker. A particular choice is

$$\phi(a) = \frac{a}{a + a_c}, \tag{39}$$

where $a_c > 0$ is a parameter that determines the growth rate of the resetting probability with a. According to the definitions in Eqs. (2) and (3), we get

$$\Phi(t) = \prod_{a=1}^{t} \left[1 - \frac{a}{a + a_c}\right] = \frac{a_c^t \Gamma(1 + a_c)}{\Gamma(1 + a_c + t)} \tag{40}$$

and

$$\Psi(t) = \frac{t}{t + a_c} \prod_{a=1}^{t-1} \left[1 - \frac{a}{a + a_c}\right] = \frac{t a_c^t \Gamma(a_c)}{\Gamma(1 + a_c + t)}, \tag{41}$$

where $\Gamma(x) = \int_0^\infty u^{x-1} e^{-u} du$ is the gamma function. Performing Laplace transform for $\Psi(t)$ and $\kappa_{ij}(t) = \Phi(t) P_{ij}^0(t)$, and combining Eq. (A3) in Appendix A given by the spectral decomposition of the transition matrix $\boldsymbol{W}$, we have

$$\tilde{\Psi}(s) = e^{-s} + (1 - e^{-s})(a_c e^{-s})^{-a_c} e^{a_c e^{-s} - s} \times \tilde{\Gamma}(1 + a_c, a_c e^{-s}) \tag{42}$$

and

$$\tilde{\kappa}_{ij}(s) = \sum_{\ell=1}^{N} \langle i|\phi_\ell\rangle \langle \bar{\phi}_\ell|j\rangle a_c e^{a_c e^{-s} \lambda_\ell} \times (a_c e^{-s} \lambda_\ell)^{-a_c} \tilde{\Gamma}(a_c, a_c e^{-s} \lambda_\ell), \tag{43}$$

where $\tilde{\Gamma}(x, y) = \int_0^y u^{x-1} e^{-u} du$ is the lower incomplete gamma function.

Substituting Eqs. (42) and (43) into Eq. (6), and then calculating the limit in Eq. (8), we obtain the stationary occupation probability of the walker in each node,

$$P_j(\infty) = \langle \bar{\phi}_1|j\rangle + \sum_{\ell=2}^{N} \frac{e^{a_c(\lambda_\ell - 1)} \lambda_\ell^{-a_c} \tilde{\Gamma}(a_c, a_c \lambda_\ell)}{\tilde{\Gamma}(a_c, a_c)} \times \langle r|\phi_\ell\rangle \langle \bar{\phi}_\ell|j\rangle. \tag{44}$$

We emphasize again that the second term in Eq. (44) is caused by the resetting.

To derive the MFPT for node i to node j, we compute $\tilde{\chi}_{ij}(0) = \sum_{t=0}^{\infty} \Phi(t) Q_{ij}^0(t)$ and $\tilde{\eta}_{ij}(0) = \sum_{t=1}^{\infty} \Psi(t) Q_{ij}^0(t-1)$ in terms of Eq. (40), Eq. (41), and the survival probability $Q_{ij}^0(t)$ in the absence of resetting [see Eq. (C3) derived in Appendix C],

$$\tilde{\chi}_{ij}(0) = \sum_{\ell=1}^{N} a_c \left(a_c \zeta_\ell^{(j)}\right)^{-a_c} e^{a_c \zeta_\ell^{(j)}} \tilde{\Gamma}\left(a_c, a_c \zeta_\ell^{(j)}\right) \times \langle i|\psi_\ell^{(j)}\rangle \langle \bar{\psi}_\ell^{(j)}|\mathbf{1}\rangle \tag{45}$$

and

$$\tilde{\eta}_{ij}(0) = \sum_{\ell=1}^{N} \left[1 + \left(a_c \zeta_\ell^{(j)}\right)^{-a_c} e^{a_c \zeta_\ell^{(j)}} \left(1 - 1/\zeta_\ell^{(j)}\right) \times \tilde{\Gamma}\left(1 + a_c, a_c \zeta_\ell^{(j)}\right)\right] \langle i|\psi_\ell^{(j)}\rangle \langle \bar{\psi}_\ell^{(j)}|\mathbf{1}\rangle. \tag{46}$$

Inserting Eqs. (45) and (46) into Eq. (13), we obtain the MFPT between two arbitrary nodes.

In Fig. 4, we compare the theory and simulation results for the anti-aging resetting protocol in Eq. (39) on a ring network of size $N = 50$ (top panels) and on a Cayley tree $C_{3,5}$ (bottom panels), where the resetting node is set to be the same as the starting node. The theoretical results are in excellent agreement with the simulation data. In Figs. 4(a) and 4(c), the stationary occupation probability at each node j is plotted as a function of the topological distance d_{rj} to the resetting node for different a_c. As expected, the walker has a larger probability to stay near the resetting node for a smaller a_c. In Figs. 4(b) and 4(d), we show the MFPT between two nodes as a function of a_c. For the ring network, we have set the distance between the starting node and the target node to $d_{ij} = 5$, and for the Cayley tree we have set the central node as the starting node and one of the outermost nodes as the target node. For both cases, the MFPT exhibits a nonmonotonic dependence on a_c. Coincidentally, the optimal a_c both appear at $a_c = 398$, at which the MFPT admits a minimum $T_{\min} = 73.167$ and $T_{\min} = 556.4$ for the ring network and the Cayley tree, respectively. The two minima of the MFPT are far less than the MFPT without resetting $\langle T_{ij}^{\text{noreset}} \rangle = d_{ij}(N - d_{ij}) = 225$ [57] and 821, and even slightly less than the minimum of the MFPT for the constant-probability resetting, that is, $T_{\min}^{\text{consreset}} = 80.274$ and 596.45 for the ring network and the Cayley tree, respectively.

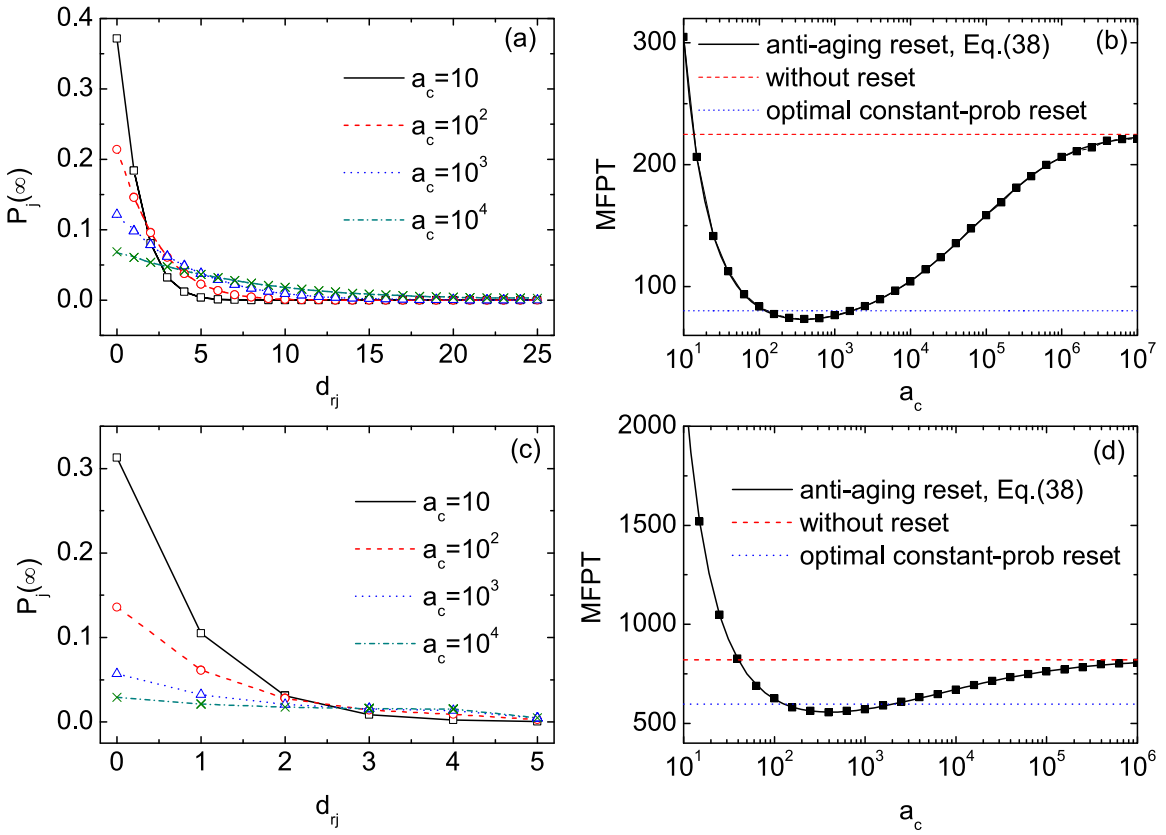

FIG. 4. Results for an anti-aging resetting [see Eq. (39)] on a ring network of $N = 50$ (top panels) and on a Cayley tree $C_{3,5}$ (bottom panels). (a) and (c) show the stationary occupation probability $P_j(\infty)$ at node j as a function of the distance d_{rj} to the resetting node r for four different values of a_c. (b) and (d) give the MFPT as a function of a_c. The resetting node is set to be the same as the starting node, $r = i$. For the ring network, the distance between the starting node and the target node is $d_{ij} = 5$. For the Cayley tree, the central node is set as the starting node, and one of the outermost nodes as the target node. Lines and symbols correspond to the theory and simulations, respectively. The dashed horizontal line in (b) and (d) indicates the value of MFPT for the case without resetting, and the dotted horizontal line indicates the minimum value of MFPT for the case of constant-probability resetting.

Finally, in Fig. 5, we present the GMFPT for the anti-aging resetting protocol on a Barbell network and a BA scale-free network, as done in the above section. For comparison, we also show the minima of the GMFPT for the constant-probability resetting, as indicated by horizontal lines in Fig. 5. For the Barbell network, the GMFPT shows a nonmonotonic

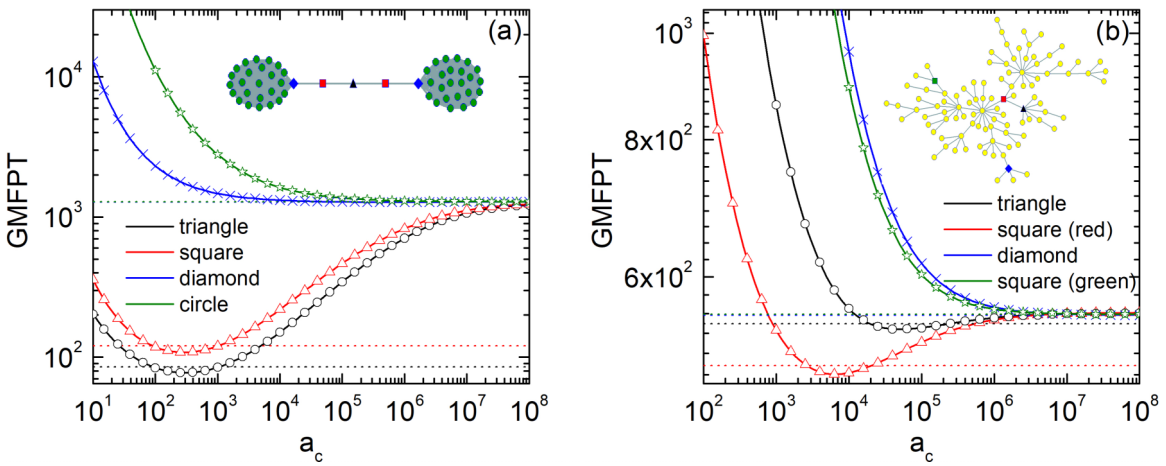

FIG. 5. Results for an anti-aging resetting [see Eq. (39)] (a) on a Barbell network of $N = 53$ and (b) on a BA scale-free network of $N = 100$. Lines and symbols correspond to the theory and simulations, respectively. The horizontal line in (a) and (b) indicates the minimal values of GMFPT for the case of constant-probability resetting.

dependence on a_c when the walker is reset to any bridge node, and a minimal GMFPT occurs at $a_c = 316$ for the midmost bridge node and at $a_c = 281$ for the remaining bridge nodes. We should note that the minimal GMFPTs in the anti-aging resetting protocol are slightly less than the counterparts in the constant-probability resetting protocol. When resetting to any node in the subgraphs, the GMFPT decreases monotonically with a_c and approaches the value without resetting as $a_c \to \infty$.

For the BA scale-free network, the GMFPT varies either monotonically or nonmonotonically with a_c, depending on which node is chosen as the resetting node. We choose four typical nodes and calculate, respectively, the GMFPT as a function of a_c, as shown in Fig. 5(b). For two interior nodes, the GMFPT shows a minimum at an intermediate value of a_c, and such a minimum is less than the minimum of GMFPT in the constant-probability resetting protocol, embodying the advantage of time-dependent resetting, while for the remaining two nodes near the periphery, the GMFPT decreases monotonically with a_c and approaches the value without resetting as $a_c \to \infty$. For the latter case, the resetting does not reduce the average time of random search, whether the resetting probability is time dependent or time independent.

VII. CONCLUSIONS

In conclusion, we have explored discrete-time random walks on networks subject to a time-dependent resetting probability to a given node. Here the resetting probability $\phi(a)$ is a function of the time a since the last reset event. We also call a the age of the walker. The present work is an extension of previous studies where the resetting probability is time independent. Using the renewal approach, we have established the formulations for the stationary occupation distribution and the MFPT between two arbitrary nodes, which are expressed in terms of the spectrum of the transition matrix and the modified transition matrix, and some resetting parameters. In particular, we consider two concrete time-dependent resetting protocols. The first one is that $\phi(a)$ is a step-shaped function of a, where the resetting probability switches from one value to another one as a crosses a threshold value a_c. The other one is that $\phi(a) = \frac{a}{a+a_c}$ is a strictly increasing function of a. Both cases are exactly solvable. Finally, we demonstrate the theoretical results on four different networks for the two resetting protocols. We find that the MFPT can be further accelerated by the time-modulated resetting probability for a wide range of a_c, compared with the constant resetting probability. Therefore, time-modulated resetting protocols are more efficient in expediting the completion of a random search process than a simple constant-probability resetting protocol.

There are still some open questions concerning the resetting paradigm. In the future, it is worth studying other types of random walks under resetting, such as biased random walks [60,93], maximum entropy random walks [94], and so on. Moreover, it would also be interesting to consider the factor of resetting costs on searching processes. In this context, how to find an optimal trade-off between the searching time cost and the resetting cost is a challenging issue [49].

ACKNOWLEDGMENTS

This work was supported by the National Natural Science Foundation of China (Grants No. 11875069 and No. 61973001).

APPENDIX A: SPECTRAL DECOMPOSITION FOR TRANSITION MATRIX WITHOUT RESETTING

For standard random walks, the transition matrix can be written as $\boldsymbol{W} = \boldsymbol{D}^{-1}\boldsymbol{A}$, where $\boldsymbol{D} = \mathrm{diag}\{k_1, \ldots, k_N\}$ is a diagonal matrix and $\boldsymbol{A}$ is the adjacency matrix of the underlying network. $\boldsymbol{W}$ can be rewritten as [58,59]

$$\boldsymbol{W} = \boldsymbol{D}^{-1/2}\tilde{\boldsymbol{A}}\boldsymbol{D}^{1/2}, \tag{A1}$$

where $\tilde{\boldsymbol{A}} = \boldsymbol{D}^{-1/2}\boldsymbol{A}\boldsymbol{D}^{-1/2}$ is a real-valued symmetric matrix for undirected networks ($\boldsymbol{A} = \boldsymbol{A}^\top$). Therefore, $\boldsymbol{W}$ is diagonalizable (i.e., spectral decomposition), and $\boldsymbol{W}$ and $\tilde{\boldsymbol{A}}$ share the same set of eigenvalues λ_ℓ ($\ell = 1, \ldots, N$) that are all real. Employing Dirac's notation, let us denote by $|v_\ell\rangle$ the right eigenvector corresponding to the ℓth eigenvalue λ_ℓ of $\tilde{\boldsymbol{A}}$. Let us denote by $\langle\bar{\phi}_\ell|$ and $|\phi_\ell\rangle$ the left eigenvector and right eigenvector of $\boldsymbol{W}$ corresponding to λ_ℓ, respectively. It is not hard to verify that $|\phi_\ell\rangle = \boldsymbol{D}^{-1/2}|v_\ell\rangle$ and $\langle\bar{\phi}_\ell| = \langle v_\ell|\boldsymbol{D}^{1/2}$.

The spectral decomposition for the transition matrix $\boldsymbol{W}$ is given by

$$\boldsymbol{W} = \sum_{\ell=1}^{N} \lambda_\ell |\phi_\ell\rangle\langle\bar{\phi}_\ell|, \tag{A2}$$

where λ_ℓ is the ℓth eigenvalue of $\boldsymbol{W}$, and the corresponding left eigenvector and right eigenvector are, respectively, $\langle\bar{\phi}_\ell|$ and $|\phi_\ell\rangle$, satisfying $\langle\bar{\phi}_\ell|\phi_m\rangle = \delta_{\ell m}$ and $\sum_{\ell=1}^{N} |\phi_\ell\rangle\langle\bar{\phi}_\ell| = \boldsymbol{I}$.

Since $\boldsymbol{W}$ is a stochastic matrix, its maximal eigenvalue is equal to one. Without loss of generality, we let $\lambda_1 = 1$ and the values of other eigenvalues are less than one. Since the sum of each row of $\boldsymbol{W}$ is equal to one, the right eigenvector corresponding to $\lambda_1 = 1$ is simply given by $|\phi_1\rangle = (1, 1, \ldots, 1)^\top$. The occupation probability $P_{ij}^0(t)$ without resetting is given by [58,59]

$$P_{ij}^0(t) = \langle i|\boldsymbol{W}^t|j\rangle = \sum_{\ell=1}^{N} \lambda_\ell^t \langle i|\phi_\ell\rangle\langle\bar{\phi}_\ell|j\rangle, \tag{A3}$$

where $|i\rangle$ denotes the canonical base with all its components equal to zero except the ith one, which is equal to one. In the limit of $t \to \infty$, all the eigenmodes decay to zero, except to the stationary eigenmode corresponding to $\lambda_1 = 1$. Therefore, we get to the occupation probability at the stationary eigenmode in the absence of resetting, $P_j^0(\infty) = \langle\bar{\phi}_1|j\rangle$.

APPENDIX B: DERIVATION OF $\tilde{Q}_{ij}^0(s)$

In the absence of resetting, the occupation probability and first passage probability satisfy the following relation [58,59]:

$$P_{ij}^0(t) = \delta_{t0}\delta_{ij} + \sum_{t'=0}^{t} F_{ij}^0(t') P_{jj}^0(t - t'), \tag{B1}$$

where $F_{ij}^0(t)$ is the first passage probability at time t in the absence of the resetting process. In the Laplace domain,

we have

$$\tilde{F}^0_{ij}(s) = \frac{\tilde{P}^0_{ij}(s) - \delta_{ij}}{\tilde{P}^0_{jj}(s)}. \tag{B2}$$

In terms of Eq. (A3), $\tilde{P}^0_{ij}(s)$ can be calculated as

$$\tilde{P}^0_{ij}(s) = \sum_{t=0}^{\infty} e^{-st} P^0_{ij}(t) = \frac{\langle\bar{\phi}_1|j\rangle}{1-e^{-s}} + \sum_{\ell=2}^{N} \frac{\langle i|\phi_\ell\rangle\langle\bar{\phi}_\ell|j\rangle}{1-\lambda_\ell e^{-s}}. \tag{B3}$$

Since $F^0_{ij}(t) = Q^0_{ij}(t-1) - Q^0_{ij}(t)$ for $t \geqslant 1$ and $F^0_{ij}(0) = 1 - Q^0_{ij}(0)$ for $t = 0$, we have $\tilde{F}^0_{ij}(s) = 1 + (e^{-s}-1)\tilde{Q}^0_{ij}(s)$. Therefore, we have

$$\tilde{Q}^0_{ij}(s) = \frac{1-\tilde{F}^0_{ij}(s)}{1-e^{-s}} = \frac{\tilde{P}^0_{jj}(s) - \tilde{P}^0_{ij}(s) + \delta_{ij}}{(1-e^{-s})\tilde{P}^0_{jj}(s)}. \tag{B4}$$

Substituting Eq. (B3) into Eq. (B4), we obtain

$$\tilde{Q}^0_{ij}(s) = \frac{\sum_{\ell=2}^{N} \frac{\langle j|\phi_\ell\rangle\langle\bar{\phi}_\ell|j\rangle - \langle i|\phi_\ell\rangle\langle\bar{\phi}_\ell|j\rangle}{1-\lambda_\ell e^{-s}} + \delta_{ij}}{\langle\bar{\phi}_1|j\rangle + (1-e^{-s})\sum_{\ell=2}^{N} \frac{\langle j|\phi_\ell\rangle\langle\bar{\phi}_\ell|j\rangle}{1-\lambda_\ell e^{-s}}}. \tag{B5}$$

Letting $s = 0$ in Eq. (B5), we obtain the mean first passage time in the absence of resetting,

$$\begin{aligned}\langle T^0_{ij}\rangle &= \tilde{Q}^0_{ij}(0) \\ &= \frac{1}{\langle\bar{\phi}_1|j\rangle}\left(\sum_{\ell=2}^{N} \frac{\langle j|\phi_\ell\rangle\langle\bar{\phi}_\ell|j\rangle - \langle i|\phi_\ell\rangle\langle\bar{\phi}_\ell|j\rangle}{1-\lambda_\ell} + \delta_{ij}\right).\end{aligned} \tag{B6}$$

APPENDIX C: DERIVATION OF $Q^0_{ij}(t)$

We will derive the expression of the survival probability in the absence of the resetting process. There is a trap located at node j, and the walker starts from node i at $t = 0$. Let us denote by $Q^0_{ij}(t)$ the survival probability, which is the probability that the walker survives up to time t. We first consider the case $i \neq j$. Let $\boldsymbol{W_j}$ be the matrix by letting all the entries in the jth row and the jth column of transition matrix $\boldsymbol{W}$ equal zero. $Q^0_{ij}(t)$ can be expressed as

$$Q^0_{ij}(t) = \sum_{k=1}^{N} \left(\boldsymbol{W_j^t}\right)_{ik}. \tag{C1}$$

For the standard random walk, the matrix $\boldsymbol{W_j}$ can be written as $\boldsymbol{W_j} = \boldsymbol{D}^{-1}\boldsymbol{A_j}$, where $\boldsymbol{D} = \mathrm{diag}\{k_1, \ldots, k_N\}$ is a diagonal matrix as before, and $\boldsymbol{A_j}$ is obtained by letting all the entries in the jth row and the jth column of the network adjacency matrix $\boldsymbol{A}$ equal zero. It is not hard to prove that $\boldsymbol{W_j}$ is diagonalizable as $\boldsymbol{W_j}$ is conjugated to a real symmetric matrix $\boldsymbol{A_j}$. Letting $\zeta^{(j)}_\ell$ be the ℓth eigenvalue of $\boldsymbol{A_j}$, and the associated eigenvector be $|u^{(j)}_\ell\rangle$, the spectral decomposition for $\boldsymbol{W_j}$ reads

$$\boldsymbol{W_j} = \sum_{\ell=1}^{N} \zeta^{(j)}_\ell |\psi^{(j)}_\ell\rangle\langle\bar{\psi}^{(j)}_\ell|, \tag{C2}$$

where $\langle\bar{\psi}^{(j)}_\ell| = \langle u^{(j)}_\ell|\boldsymbol{D}^{1/2}$ and $|\psi^{(j)}_\ell\rangle = \boldsymbol{D}^{-1/2}|u^{(j)}_\ell\rangle$ are, respectively, the left eigenvector and right eigenvector of $\boldsymbol{W_j}$ corresponding to the ℓth eigenvalue, satisfying $\langle\bar{\psi}^{(j)}_\ell|\psi^{(j)}_m\rangle = \delta_{\ell m}$ and $\sum_{\ell=1}^{N} |\psi^{(j)}_\ell\rangle\langle\bar{\psi}^{(j)}_\ell| = \boldsymbol{I}$. Since the sum of each row of $\boldsymbol{W_j}$ is always less than or equal to one, the eigenvalues $\zeta^{(j)}_\ell$ are strictly less than one.

According to Eq. (C2), the survival probability can be computed by

$$Q^0_{ij}(t) = \sum_{k=1}^{N}\sum_{\ell=1}^{N} \left(\zeta^{(j)}_\ell\right)^t \langle i|\psi^{(j)}_\ell\rangle\langle\bar{\psi}^{(j)}_\ell|k\rangle \quad \text{for} \quad i \neq j. \tag{C3}$$

If the target is located at the starting node, $Q^0_{ii}(t)$ is the probability that the walker does not return to the original node. We define $Q^0_{ii}(t=0) = 0$ and, for $t \geqslant 1$,

$$Q^0_{ii}(t) = \sum_{j=1}^{N}\sum_{k=1}^{N} W_{ij}\left(\boldsymbol{W_i^{t-1}}\right)_{jk}. \tag{C4}$$

According to Eq. (C2), $Q^0_{ii}(t)$ for $t \leqslant 1$ is written as

$$Q^0_{ii}(t) = \sum_{j=1}^{N}\sum_{k=1}^{N}\sum_{\ell=1}^{N} W_{ij}\left(\zeta^{(i)}_\ell\right)^{t-1}\langle j|\psi^{(i)}_\ell\rangle\langle\bar{\psi}^{(i)}_\ell|k\rangle. \tag{C5}$$

[1] M. R. Evans and S. N. Majumdar, Phys. Rev. Lett. **106**, 160601 (2011).
[2] M. R. Evans, S. N. Majumdar, and G. Schehr, J. Phys. A: Math. Theor. **53**, 193001 (2020).
[3] M. R. Evans and S. N. Majumdar, J. Phys. A: Math. Theor. **44**, 435001 (2011).
[4] S. Eule and J. J. Metzger, New J. Phys. **18**, 033006 (2016).
[5] A. Pal, A. Kundu, and M. R. Evans, J. Phys. A: Math. Theor. **49**, 225001 (2016).
[6] A. Nagar and S. Gupta, Phys. Rev. E **93**, 060102(R) (2016).
[7] V. P. Shkilev, Phys. Rev. E **96**, 012126 (2017).
[8] L. Kuśmierz and T. Toyoizumi, Phys. Rev. E **100**, 032110 (2019).
[9] M. R. Evans and S. N. Majumdar, J. Phys. A: Math. Theor. **47**, 285001 (2014).
[10] C. Christou and A. Schadschneider, J. Phys. A: Math. Theor. **48**, 285003 (2015).
[11] V. Domazetoski, A. Masó-Puigdellosas, T. Sandev, V. Méndez, A. Iomin, and L. Kocarev, Phys. Rev. Res. **2**, 033027 (2020).
[12] P. C. Bressloff, J. Stat. Mech. (2021) 063206.
[13] H. Chen and F. Huang, Phys. Rev. E **105**, 034109 (2022).
[14] M. R. Evans and S. N. Majumdar, J. Phys. A: Math. Theor. **52**, 01LT01 (2019).
[15] A. Pal, L. Kuśmierz, and S. Reuveni, New J. Phys. **21**, 113024 (2019).
[16] A. S. Bodrova and I. M. Sokolov, Phys. Rev. E **101**, 052130 (2020).

[17] D. Gupta, C. A. Plata, A. Kundu, and A. Pal, J. Phys. A: Math. Theor. **54**, 025003 (2021).
[18] A. Pal, Phys. Rev. E **91**, 012113 (2015).
[19] S. Ahmad, I. Nayak, A. Bansal, A. Nandi, and D. Das, Phys. Rev. E **99**, 022130 (2019).
[20] M. R. Evans and S. N. Majumdar, J. Phys. A: Math. Theor. **51**, 475003 (2018).
[21] I. Santra, U. Basu, and S. Sabhapandit, J. Stat. Mech. (2020) 113206.
[22] P. C. Bressloff, Phys. Rev. E **102**, 042135 (2020).
[23] A. Scacchi and A. Sharma, Mol. Phys. **116**, 460 (2018).
[24] V. Kumar, O. Sadekar, and U. Basu, Phys. Rev. E **102**, 052129 (2020).
[25] B. De Bruyne, S. N. Majumdar, and G. Schehr, Phys. Rev. Lett. **128**, 200603 (2022).
[26] U. Basu, A. Kundu, and A. Pal, Phys. Rev. E **100**, 032136 (2019).
[27] S. Reuveni, Phys. Rev. Lett. **116**, 170601 (2016).
[28] A. Pal and S. Reuveni, Phys. Rev. Lett. **118**, 030603 (2017).
[29] S. Gupta, S. N. Majumdar, and G. Schehr, Phys. Rev. Lett. **112**, 220601 (2014).
[30] J. M. Meylahn, S. Sabhapandit, and H. Touchette, Phys. Rev. E **92**, 062148 (2015).
[31] A. Chechkin and I. M. Sokolov, Phys. Rev. Lett. **121**, 050601 (2018).
[32] S. N. Majumdar, F. Mori, H. Schawe, and G. Schehr, Phys. Rev. E **103**, 022135 (2021).
[33] B. De Bruyne, J. Randon-Furling, and S. Redner, Phys. Rev. Lett. **125**, 050602 (2020).
[34] M. Magoni, S. N. Majumdar, and G. Schehr, Phys. Rev. Res. **2**, 033182 (2020).
[35] M. Biroli, F. Mori, and S. N. Majumdar, J. Phys. A: Math. Theor. **55**, 244001 (2022).
[36] A. Pal, S. Kostinski, and S. Reuveni, J. Phys. A: Math. Theor. **55**, 021001 (2022).
[37] P. Singh and A. Pal, J. Phys. A: Math. Theor. **55**, 234001 (2022).
[38] J. Fuchs, S. Goldt, and U. Seifert, Europhys. Lett. **113**, 60009 (2016).
[39] A. Pal and S. Rahav, Phys. Rev. E **96**, 062135 (2017).
[40] D. Gupta, C. A. Plata, and A. Pal, Phys. Rev. Lett. **124**, 110608 (2020).
[41] S. Reuveni, M. Urbakh, and J. Klafter, Proc. Natl. Acad. Sci. USA **111**, 4391 (2014).
[42] D. Boyer and C. Solis-Salas, Phys. Rev. Lett. **112**, 240601 (2014).
[43] T. Rotbart, S. Reuveni, and M. Urbakh, Phys. Rev. E **92**, 060101(R) (2015).
[44] O. Vilk, D. Campos, V. Méndez, E. Lourie, R. Nathan, and M. Assaf, Phys. Rev. Lett. **128**, 148301 (2022).
[45] M. R. Evans, S. N. Majumdar, and G. Schehr, J. Phys. A: Math. Theor. **55**, 274005 (2022).
[46] P. Singh and A. Pal, Phys. Rev. E **103**, 052119 (2021).
[47] C. Godréche and J.-M. Luck, J. Stat. Mech. (2022) 063202.
[48] S. N. Majumdar, P. Mounaix, S. Sabhapandit, and G. Schehr, J. Phys. A: Math. Theor. **55**, 034002 (2022).
[49] B. D. Bruynea and F. Mori, arXiv:2112.11416.
[50] O. Tal-Friedman, A. Pal, A. Sekhon, S. Reuveni, and Y. Roichman, J. Phys. Chem. Lett. **11**, 7350 (2020).
[51] B. Besga, A. Bovon, A. Petrosyan, S. N. Majumdar, and S. Ciliberto, Phys. Rev. Res. **2**, 032029(R) (2020).
[52] K. Avrachenkov, R. Van Der Hofstad, and M. Sokol, in *International Workshop on Algorithms and Models for the Web-Graph*, edited by A. Bonato, F. C. Graham, and P. Prałat (Springer, Cham, Switzerland, 2014), pp. 23–33.
[53] K. Avrachenkov, A. Piunovskiy, and Y. Zhang, Methodol. Comput. Appl. Probab. **20**, 1173 (2018).
[54] L. Christophorov, J. Phys. A: Math. Theor. **54**, 015001 (2021).
[55] S. Wald and L. Böttcher, Phys. Rev. E **103**, 012122 (2021).
[56] O. L. Bonomo and A. Pal, Phys. Rev. E **103**, 052129 (2021).
[57] F. Huang and H. Chen, Phys. Rev. E **103**, 062132 (2021).
[58] N. Masuda, M. A. Porter, and R. Lambiotte, Phys. Rep. **716-717**, 1 (2017).
[59] J. D. Noh and H. Rieger, Phys. Rev. Lett. **92**, 118701 (2004).
[60] Z. Zhang, T. Shan, and G. Chen, Phys. Rev. E **87**, 012112 (2013).
[61] R. Pastor-Satorras, C. Castellano, P. Van Mieghem, and A. Vespignani, Rev. Mod. Phys. **87**, 925 (2015).
[62] V. Colizza, R. Pastor-Satorras, and A. Vespignani, Nat. Phys. **3**, 276 (2007).
[63] V. Belik, T. Geisel, and D. Brockmann, Phys. Rev. X **1**, 011001 (2011).
[64] M. Assaf and B. Meerson, J. Phys. A: Math. Theor. **50**, 263001 (2017).
[65] J. Hindes and I. B. Schwartz, Phys. Rev. Lett. **117**, 028302 (2016).
[66] H. C. Tuckwell, *Introduction to Theoretical Neurobiology: Volume 2, Nonlinear and Stochastic Theories*, No. 8 (Cambridge University Press, Cambridge, 1988).
[67] V. Sood and S. Redner, Phys. Rev. Lett. **94**, 178701 (2005).
[68] M. Rosvall and C. T. Bergstrom, Proc. Natl. Acad. Sci. USA **105**, 1118 (2008).
[69] H. Zhou and R. Lipowsky, in *International Conference on Computational Science*, edited by M. Bubak, G. D. van Albada, P. M. A. Sloot, and J. Dongarra (Springer, Berlin, Heidelberg, 2004), pp. 1062–1069.
[70] P. Pons and M. Latapy, in *International Symposium on Computer and Information Sciences*, edited by P. Yolum, C. Özturan, T. Güngör, and F. Gürgen (Springer, Berlin, Heidelberg, 2005), pp. 284–293.
[71] L. Prignano, Y. Moreno, and A. Díaz-Guilera, Phys. Rev. E **86**, 066116 (2012).
[72] A. Riascos and J. L. Mateos, PLoS One **12**, e0184532 (2017).
[73] H. Barbosa, M. Barthelemy, G. Ghoshal, C. R. James, M. Lenormand, T. Louail, R. Menezes, J. J. Ramasco, F. Simini, and M. Tomasini, Phys. Rep. **734**, 1 (2018).
[74] M. E. Newman, Social Networks **27**, 39 (2005).
[75] L. Lü, D. Chen, X.-L. Ren, Q.-M. Zhang, Y.-C. Zhang, and T. Zhou, Phys. Rep. **650**, 1 (2016).
[76] J. Kleinberg, in *Proceedings of the International Congress of Mathematicians (ICM)* (European Mathematical Society, Madrid, Spain, 2006), Vol. 3, pp. 1019–1044.
[77] L. Ermann, K. M. Frahm, and D. L. Shepelyansky, Rev. Mod. Phys. **87**, 1261 (2015).
[78] E. Bautista, P. Abry, and P. Gonçalves, Appl. Network Sci. **4**, 57 (2019).
[79] S. Brin and L. Page, Comput. Netw. ISDN Syst. **30**, 107 (1998).
[80] M. C. González, C. A. Hidalgo, and A.-L. Barabasi, Nature (London) **453**, 779 (2008).
[81] P. D. Walsh, D. Boyer, and M. C. Crofoot, Nat. Phys. **6**, 929 (2010).

[82] O. Bénichou, C. Loverdo, M. Moreau, and R. Voituriez, Rev. Mod. Phys. **83**, 81 (2011).
[83] A. P. Riascos, D. Boyer, P. Herringer, and J. L. Mateos, Phys. Rev. E **101**, 062147 (2020).
[84] D. C. Rose, H. Touchette, I. Lesanovsky, and J. P. Garrahan, Phys. Rev. E **98**, 022129 (2018).
[85] A. P. Riascos, D. Boyer, and J. L. Mateos, J. Phys. A: Math. Theor. **55**, 274002 (2022).
[86] F. H. González, A. P. Riascos, and D. Boyer, Phys. Rev. E **103**, 062126 (2021).
[87] S. Wang, H. Chen, and F. Huang, Chaos **31**, 093135 (2021).
[88] Y. Ye and H. Chen, J. Stat. Mech. (2022) 053201.
[89] A. Ghosh, S. Boyd, and A. Saberi, SIAM Rev. **50**, 37 (2008).
[90] A.-L. Barabási and R. Albert, Science **286**, 509 (1999).
[91] P. Erdös and A. Rényi, Publ. Math. Inst. Hung. Acad. Sci **5**, 17 (1960).
[92] D. J. Watts and S. H. Strogatz, Nature (London) **393**, 440 (1998).
[93] Y. Lin and Z. Zhang, Phys. Rev. E **87**, 062140 (2013).
[94] Z. Burda, J. Duda, J. M. Luck, and B. Waclaw, Phys. Rev. Lett. **102**, 160602 (2009).